Progress In Electromagnetics Research Letters, Vol. 110, 83–91, 2023

Design and Analysis of S-Shaped Broadside Coupled Metamaterial Unit Cell as a Sensor to Ease the Classification of Different Oil Samples

Jeyagobi Logeswaran* **and Rajasekar Boopathi Rani**

Abstract—This paper aims to classify oil samples using metamaterial (MTM) unit cell as a sensor. An S-shaped broadside coupled Split-Ring Resonator (SRR) acts as an MTM and is designed to operate at X-band (8–12.4 GHz). The proposed MTM unit cell was simulated through the High Frequency EM simulation tool, and then the MTM properties were extracted using the standard equations. The MTM behavior was studied through its negative permittivity and permeability characteristics in the X-band. The simulated and extracted properties exhibit that the proposed MTM unit cell is suitable for the analysis at X-band. A sample container was designed to hold different oil samples. The experimental analysis was carried out by filling the container with different oils without/with an MTM sensor. Mainly, the variations in S-parameters magnitude were studied for classification applications. This paper proposes the study of transmission coefficients phase response in addition to magnitude as an easy way to classify different oils. Further, the phase transition results were compared with the kinematic viscosity and refractive index properties of the oil sample. The comparison results proved that the classification of oil samples using the phase transition approach agrees well with the existing oil properties.

1. INTRODUCTION

Oil is an integral part of human's daily activities. There are different kinds of oil available in the market such as castor oil, neem oil, sunflower oil, sesame oil, and mahua oil. The usage of a particular oil will differ from one region to another region of the country, and it also depends on the age group of the people. Hence, it is essential to classify different types of oil. The goal of this work is to create a low-cost, simple-to-use sensor structure that can distinguish between different oils.

The classification can be carried out by studying the variations in S-parameter characteristics by keeping the Material Under Test (MUT) in between the input and output ports of a microwave bench. In this measurement setup, the inclusion of some resonant structure will improve the classification accuracy and ease the process. Metamaterial (MTM) is one type of resonant structures which finds applications in many fields such as sensors [1, 2], antennas [3], and absorbers [4]. MTMs are artificially made materials which have negative permittivity and permeability characteristics. MTM structure can be used to distinguish different types of oils too. The MTM's properties mainly depend on its shape, dimensions, and orientation of the unit cell. The classification can be carried out by studying the shift in resonance and its peak. This kind of studies has already been reported in literature to detect the glucose intensity in aqueous solution [5], water quality measurement [6], measuring the alcohol ratio [7], and detection of adulterated fuel [9]. Split Ring Resonators (SRRs) are the most commonly used MTM structure due to their simple geometry and suitability to a wide range of applications. Hence, the

Received 25 January 2023, Accepted 29 April 2023, Scheduled 9 May 2023
* Corresponding author: Jeyagobi Logeswaran (logeswaranjg@gmail.com).
The authors are with the Department of ECE, National Institute of Technology Puducherry Karaikal, Puducherry UT, India.

proposed MTM structure is based on the S-shaped SRR MTM structure on both sides of the substrate. This structure couples signals in broadside and improves the classification accuracy. In this paper, the S-shaped Broadside Coupled (BC) SRR is designed and proposed for oil classification applications. The paper is organized as follows. Sections 2 and 3 present the design of the MTM structure and its properties extraction, respectively. Section 4 presents the experimental setup and procedures. Section 5 presents the analysis for oil classification. Section 6 presents the comparison of the proposed work with the literature. Finally, Section 7 provides the conclusion.

2. DESIGN OF METAMATERIAL (MTM) STRUCTURE

Figure 1(a) shows the 3D view of the proposed BC-MTM structure, which is used to sense the characteristics of different oil samples. The MTM structure was simulated using the High Frequency Structure Simulator (HFSS). The proposed MTM structure comprises S-shaped copper strips affixed on both sides of the Flame Retardant 4 (FR4) dielectric substrate. The advantages of using an FR4 dielectric substrate are low-profile, being economical, and high mechanical strength. The FR4 dielectric properties include its relative permittivity (ε_r) of 4.4 and loss tangent of 0.02. The thickness of the FR4 dielectric substrate is 1.6 mm. The copper strip has a conductivity of 5.8×10^7 S/m and a thickness of 0.035 mm. The proposed MTM structure was placed between the two X-band waveguides for the experimental analysis. Hence, the dimension of the proposed MTM structure's substrate is compatible with the specifications of WR90. The geometry of the proposed MTM structure is shown in Figure 1(b), and the dimensions are listed in Table 1.

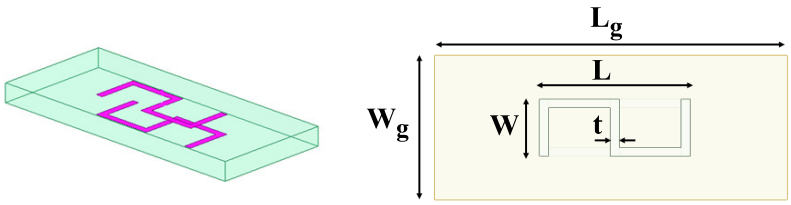

Figure 1. (a) 3D view & (b) geometry of the proposed MTM structure.

Table 1. Dimensions of the proposed MTM structure.

Parameters	L_g	W_g	L	W	t
Value (mm)	22.86	10.16	9.80	4.00	0.60

3. EXTRACTION OF MTM PROPERTY

The simulated reflection coefficient (S_{11}) and transmission coefficient (S_{21}) magnitude responses of the proposed MTM structure are depicted in Figure 2. From the responses, it can be observed that the minimum S_{21} value of -26.28 dB is obtained at 8.6 GHz, and the minimum S_{11} value of -22.84 dB is obtained at 10 GHz. Hence, the responses of the proposed MTM structure are present within the range of X-band, and it can also be used to classify the different types of oil samples through a waveguide medium.

Even though the minimum S_{11} and S_{21} responses are within the X-band range, the MTM property can be validated by the effective permittivity and permeability characteristics. The real and imaginary parts of the permittivity and permeability of the proposed MTM structure were extracted using the standard equations [8]. The permittivity (ε) and permeability (μ) of the MTM structure are calculated using Equations (1) and (2) [8].

$$\varepsilon = \frac{n}{z} \tag{1}$$

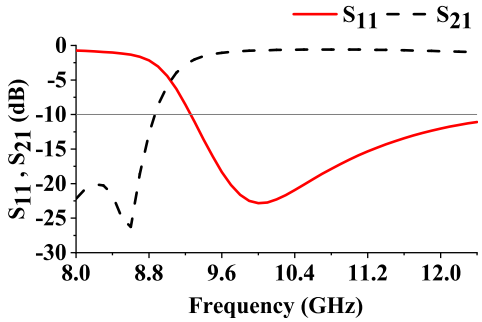

Figure 2. S_{11} & S_{21} response of the proposed MTM structure.

$$\mu = nz \tag{2}$$

where n is the refractive index, and z is the impedance presented by the MTM. They are related to S-parameters as presented in Equations (3) and (4) [8].

$$z = \sqrt{\frac{(1+S_{11})^2 - S_{21}^2}{(1-S_{11})^2 - S_{21}^2}} \tag{3}$$

$$n = \frac{1}{kd}\cos^{-1}\left[\frac{(1-S_{11}^2+S_{21}^2)}{2S_{21}}\right] \tag{4}$$

In Equation (4), S_{11} and S_{21} represent the reflection and transmission coefficients of the MTM structure; k represents the wave number; and d represents a larger dimension of the MTM structure which is the length of the substrate (L_g). From Figure 3, it can be inferred that the negative values for real permittivity were observed over the frequency range from 12.1 GHz to 12.4 GHz, and for real permeability they were observed over the range from 9.2 GHz to 10.8 GHz. Hence, the proposed structure exhibits MTM property in the X-band range.

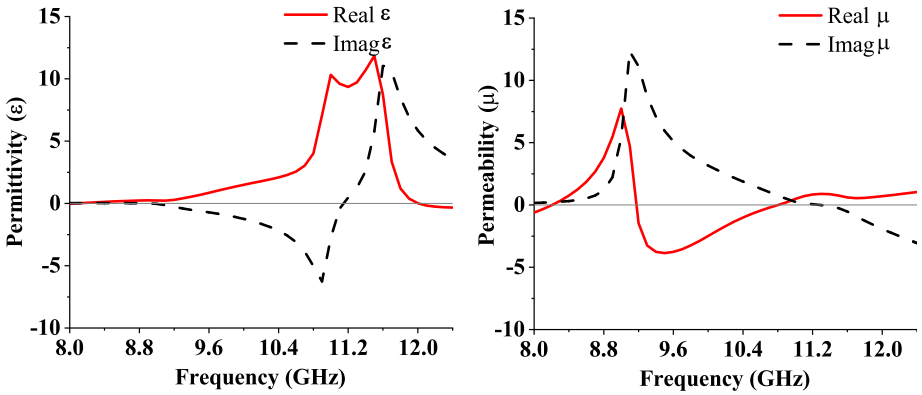

Figure 3. (a) Permittivity & (b) permeability of the proposed MTM structure.

4. EXPERIMENTAL SETUP

Figures 4(a) and 4(b) depict front and back views of the proposed MTM structure, and the experimental setup is shown in Figure 4(c). As the MTM was designed and validated at X-band frequency region, the setup has also been designed using X-band microwave bench and Vector Network Analyzer (VNA). A sample container is used to hold oil samples under test. The sample container was made using the

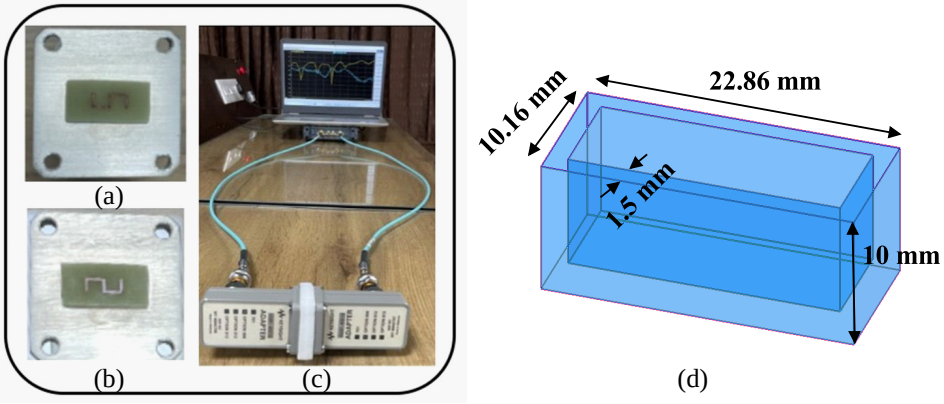

Figure 4. (a) Front view. (b) Back view. (c) Experimental setup of the MTM based structure. (d) 3D view of the sample container.

epoxy adhesive compound. The important features of the sample container are the ability to withstand constant weight or force over an extended period and good resistance to the physical and chemical influences of the sample. The geometry of the sample container is depicted in Figure 4(d).

5. ANALYSIS ON THE CLASSIFICATION OF DIFFERENT OIL SAMPLES

In general, each oil has a distinct quality and application. This quality and application are based on its ingredients and physical nature. The primary purposes behind the oil are cooking, bio-diesel, herbal, etc. Hence, it is essential to classify the oils. For this purpose, the proposed MTM sensor was used and classified the following oil samples. The samples are castor oil, neem oil, sunflower oil, sesame oil, and mahua oil. The characteristics of the oil samples were studied using the S_{11} and S_{21} responses. The importance of the proposed MTM structure was analyzed by comparing the measurement results without and with the MTM structure.

5.1. Analysis Using *S*-Parameter's Magnitude Response without and with MTM Structure

In Figures 5 & 6, the experimental analysis was carried out without/with MTM structure, and the corresponding S_{11} and S_{21} responses were observed using VNA. A detailed inference is made in Table 2. The detailed inference about the frequency shift and analysis with the MTM structure can be inferred from Table 2.

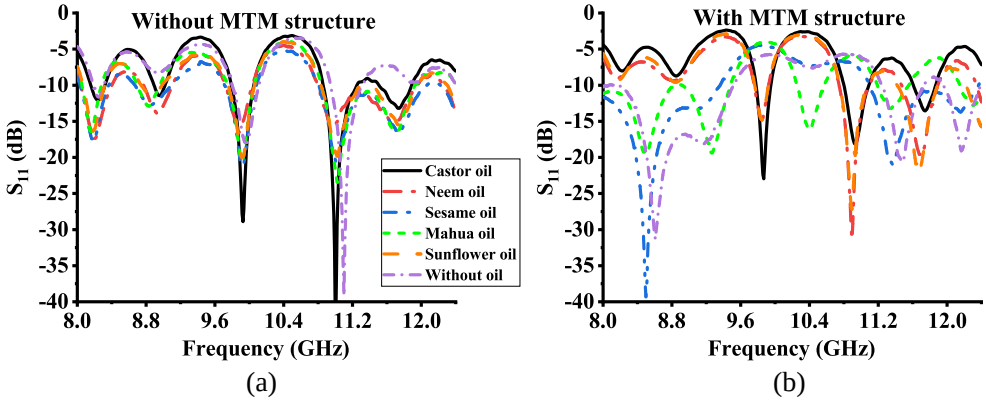

Figure 5. S_{11} response without/with MTM structure.

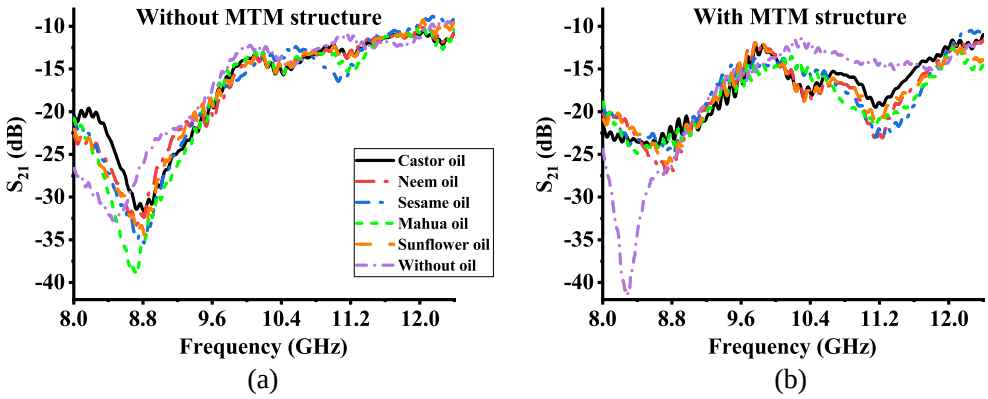

Figure 6. S_{21} response without/with MTM structure.

Table 2. S-parameters magnitude response for the different oil samples without/with the MTM structure.

Classification type	Parameter		Castor oil	Neem oil	Sunflower oil	Sesame oil	Mahua oil
Without MTM	$\|S_{11}\|$	Freq. (GHz)	11.00	10.94	11.02	11.02	11.02
		Value (dB)	−45.29	−15.72	−19.83	−22.73	−21.03
	$\|S_{21}\|$	Freq. (GHz)	8.72	8.72	8.74	8.72	8.72
		Value (dB)	−31.44	−33.35	−34.44	−39.08	−35.02
With MTM	$\|S_{11}\|$	Freq. (GHz)	11.75	11.70	11.67	11.34	11.37
		Value (dB)	−13.56	−19.87	−22.27	−13.23	−20.99
	$\|S_{21}\|$	Freq. (GHz)	8.54	8.63	8.73	8.40	8.81
		Value (dB)	−24.00	−26.54	−26.11	−24.88	−25.06

From Table 2, the observed inferences are:

i) Without MTM structure

a) Even though oil properties are unique, there is no noticeable shift in S_{11} resonance frequency between oils such as sunflower oil, sesame oil, and mahua oil at 11.02 GHz.

b) The various oils have similar S_{21} peak resonance frequencies, which made it difficult to classify oil. There is no frequency shift in the S_{21} response of oil samples such as castor oil, neem oil, sesame oil, and mahua oil.

Hence, it is difficult to classify oils only with a simple container between waveguides.

ii) With MTM structure

a) The S_{11} resonance frequency shift was observed in the frequency range of 11.34 GHz to 11.75 GHz for different oil samples. The minimum frequency shift between any two oil samples (sesame oil and mahua oil) is at least more than 30 MHz, and the maximum frequency shift between the sesame oil and castor oil is 410 MHz.

b) The S_{21} resonance frequency shift was observed in the frequency range of 8.40 GHz to 8.81 GHz for different oil samples. The minimum frequency shift between any two oil samples (castor oil and neem oil) is at least more than 90 MHz, and the maximum frequency shift between the sesame oil and mahua oil is 410 MHz.

Hence, different oils can be easily classified with maximum accuracy using a sample container with an MTM structure.

5.2. Analysis Using *S*-Parameter's Phase Response without and with MTM Structure

Figure 7 shows the S_{21} phase responses of different oil samples without and with MTM structure. The S_{21} phase transition frequency, kinematic viscosity, and refractive index of the various oil samples are listed in Table 3. The phase transition frequency was observed without/with the proposed MTM structure. The kinematic viscosity and refractive index values of different oil samples were referred from existing literature [15, 16] and provided in Table 3. Some inferences are shown in Table 3.

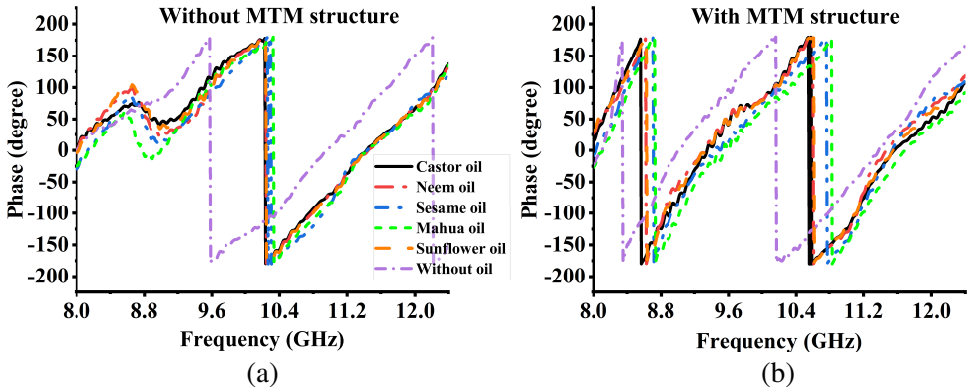

Figure 7. S_{21} phase response without/with MTM structure.

Table 3. Comparison of properties of oil sample with S_{21} phase transition frequency.

S.No	Type of oil sample	S_{21} phase transition frequency			kinematic viscosity at 40°c (cSt)	Refractive Index
		without MTM structure (GHz)	with MTM structure (GHz)			
1.	Castor oil	10.24	8.57	10.55	13.50	1.4700–1.4740
2.	Neem oil	10.25	8.63	10.60	32.27	1.4650–1.4705
3.	Sunflower oil	10.25	8.64	10.61	33.90	1.4640–1.4691
4.	Sesame oil	10.27	8.71	10.78	35.50	1.4646–1.4665
5.	Mahua oil	10.33	8.73	10.84	37.63	1.4590–1.4611

a) Without the proposed MTM structure, −180° to 180° phase transition occurs at different frequencies of range from 10.24 to 10.33 GHz. Oils such as neem and sunflower have a transition at the same frequency of 10.25 GHz. It leads to difficulty in the classification of these oils.

b) With the proposed MTM structure, there were two phase transitions observed in X-band range. One phase transition occurs in the frequency range from 8.57 to 8.73 GHz, and the other transition is from 10.55 to 10.84 GHz with minimum frequency variations of 10 MHz between different oils.

c) The oil property can also be studied using the kinematic viscosity and refractive index value. The corresponding oil property values are arranged in order. It clearly indicates the relationship between the phase transition frequency and oil properties. When the kinematic viscosity value increases, phase transition frequency also increases. It is also inferred that the decrease in refractive index value causes an increase in phase transition frequency.

The consolidated $|S_{11}|$, $|S_{21}|$, and S_{21} phase transition responses of the proposed MTM structure with different oil samples are shown in Table 4. The following inferences are made from Table 4:

Table 4. Consolidation of observed variations in S-parameter properties for different oil samples.

S.No	Type of oil sample	Reflection coefficient ($\|S_{11}\|$)		Transmission coefficient ($\|S_{21}\|$)		S_{21} phase transition frequency (GHz)	
		Freq. (GHz)	Value (dB)	Freq. (GHz)	Value (dB)	1st transition	2nd transition
1.	Castor oil	11.75	−13.56	8.54	−24.00	8.57	10.55
2.	Neem oil	11.70	−19.87	8.63	−26.54	8.63	10.60
3.	Sunflower oil	11.67	−22–27	8.73	−26.11	8.64	10.61
4.	Sesame oil	11.34	−13.23	8.40	−24.88	8.71	10.78
5.	Mahua oil	11.37	−20.99	8.81	−25.06	8.73	10.84

a) Sesame oil has minimum $|S_{11}|$ at a lower frequency of 11.34 GHz, and sunflower oil has a lower value of $|S_{11}|$ than other oil samples in the range of analysis from 11 to 12 GHz. Hence, the lower resonance frequency range and lower $|S_{11}|$ values may suit for identifying cooking oil applications.

b) Castor oil has $|S_{11}|$ resonance at a higher frequency of 11.75 GHz with a higher $|S_{11}|$ value, and mahua oil has $|S_{11}|$ resonance at a lower frequency of 11.37 GHz with a lower $|S_{11}|$ value in the range of analysis form 11 to 12 GHz. Hence, this type of oil may suit for identifying bio-diesel oils.

c) Neem oil has $|S_{11}|$ resonance frequency of 11.67 GHz in the middle of four different oil's resonance frequencies, and it may suit for identifying herbal oil.

d) The peak $|S_{21}|$ observed for different oil samples are almost the same. The classification can be made by analyzing the S_{21} phase response, which is already detailed in Table 3.

6. COMPARISON OF THE PROPOSED WORK WITH OTHER EXISTING WORKS

The comparison between the proposed work and existing works in terms of material sensed, the parameters used for sensing, and the minimum observed shift is listed in Table 5. From Table 5, it can be observed that the proposed work has three sensing parameters i.e., $|S_{11}|$, $|S_{21}|$, and S_{21} phase transitions. The oil classification based on $|S_{11}|$ response has frequency shift ranging from a minimum of 30 MHz to a maximum of 410 MHz between the oil samples under test. Hence, it can further improve

Table 5. Comparison of the proposed work with other existing works.

Ref.	Material Sensed	Sensing Parameter	Resonance frequency shift (MHz)
[9]	Diesel	$\|S_{21}\|$	60
[10]	Diesel	$\|S_{11}\|$	120
[11]	Transformer oil and Lubricant oil	$\|S_{21}\|$	60–70
[12]	Olive oil and Cotton oil	$\|S_{11}\|$	150
[13]	Gasoline	$\|S_{11}\|$	28
[14]	Olive oil, Corn oil, Sunflower oil, Palm oil, Brake oil, Benzene, Carbon-tetrachloride	$\|S_{11}\|$	70–100
This Work	Castor oil, Neem oil, Sunflower oil, Sesame oil and Mahua oil	$\|S_{11}\|$	30
		$\|S_{21}\|$	90
		Phase transition	10

the classification of different oil samples, and also the sensing based on the $|S_{21}|$ parameter is better than the existing literature [9, 11]. The S_{21} phase transition responses hold a good agreement with the other properties of oil such as kinematic viscosity and refractive index value. These factors lead to the effective classification of oil samples.

7. CONCLUSION

The proposed MTM structure was used to classify oil samples such as castor oil, neem oil, sunflower oil, sesame oil, and mahua oil. The classification of oil samples was done without/with MTM structure. From the experimental analysis, it can be observed that the oil samples tested with an MTM structure have greater significance in classification than those without MTM structures. The phase transition values also hold a good match with the other oil properties such as kinematic viscosity and refractive index value. Hence, the proposed sensor and methods are viable to be used in the classification of different oil samples.

ACKNOWLEDGMENT

The authors would like to express their acknowledgment to the National Institute of Technology Puducherry, Karaikal, for providing the necessary resources and support for this research.

REFERENCES

1. Malena, L., O. Fiser, P. R. Stauffer, T. Drizdal, J. Vrba, and D. Vrba, "Feasibility evaluation of metamaterial microwave sensors for non-invasive blood glucose monitoring," *Sensors*, Vol. 21, No. 20, 6871, 2021.
2. Islam, M. R., M. T. Islam, A. Hoque, M. S. Soliman, B. Bais, N. M. Sahar, and S. H. A. Almalki, "Tri circle split ring resonator shaped metamaterial with mathematical modeling for oil concentration sensing," *IEEE Access*, Vol. 9, 161087–161102, 2021.
3. Lee, W., S.-I. Choi, H.-I. Kim, S. Hwang, S. Jeon, and Y.-K. Yoon, "Metamaterial-integrated high-gain rectenna for RF sensing and energy harvesting applications," *Sensors*, Vol. 21, No. 19, 6580, 2021.
4. Abdulkarim, Y. I., L. Deng, O. Altıntaş, E. Ünal, and M. Karaaslan, "Metamaterial absorber sensor design by incorporating swastika shaped resonator to determination of the liquid chemicals depending on electrical characteristics," *Physica E: Low-dimensional Systems and Nanostructures*, Vol. 114, 113593, 2019.
5. Islam, M. T., A. Hoque, A. F. Almutairi, and N. Amin, "Left-handed metamaterial-inspired unit cell for S-band glucose sensing application," *Sensors*, Vol. 19, No. 1, 169, 2019.
6. Logeswaran, J. and R. B. Rani, "UWB antenna as a sensor for the analysis of dissolved particles and water quality," *Progress In Electromagnetics Research Letters*, Vol. 106, 31–39, 2022.
7. Ahmed, K., M. J. Haque, M. A. Jabin, B. K. Paul, I. S. Amiri, and P. Yupapin, "Tetra-core surface plasmon resonance based biosensor for alcohol sensing," *Physica B: Condensed Matter*, Vol. 570, 2019.
8. Smith, D. R., D. C. Vier, Th. Koschny, and C. M. Soukoulis, "Electromagnetic parameter retrieval from inhomogeneous metamaterials," *Physical Review E*, Vol. 71, No. 3, 036617, 2005.
9. Tamer, A., F. Karadağ, E. Ünal, Y. I. Abdulkarim, L. Deng, O. Altintas, M. Bakır, and M. Karaaslan, "Metamaterial based sensor integrating transmission line for detection of branded and unbranded diesel fuel," *Chemical Physics Letters*, Vol. 742, 137169, 2020.
10. Abdulkarim, Y. I., L. Deng, M. Karaaslan, Ş. Dalgaç, R. H. Mahmud, F. Ozkan Alkurt, F. F. Muhammadsharif, H. N. Awl, S. Huang, and H. Luo, "The detection of chemical materials with a metamaterial-based sensor incorporating oval wing resonators," *Electronics*, Vol. 9, 825, 2020.

11. Altıntaş, O., M. Aksoy, and E. Ünal, "Design of a metamaterial inspired omega shaped resonator based sensor for industrial implementations," *Physica E: Low-dimensional Systems and Nanostructures*, Vol. 116, 2020.
12. Bakır, M., Ş. Dalgaç, M. Karaaslan, F. Karadağ, O. Akgol, E. Unal, T. Depci, and C. Sabah, "A comprehensive study on fuel adulteration sensing by using triple ring resonator type metamaterial," *Journal of the Electrochemical Society*, Vol. 166, B1044–B1052, 2019.
13. Tümkaya, M. A., E. Ünal, and C. Sabah, 'Metamaterial-based fuel sensor application with three rhombus slots," *International Journal of Modern Physics B*, Vol. 33, 2019.
14. Islam, M. R., M. T. Islam, B. Bais, S. H. A. Almalki, and H. Alsaif, "Metamaterial sensor based on rectangular enclosed adjacent triple circle split ring resonator with good quality factor for microwave sensing application," *Scientific Reports*, Vol. 12, No. 1, 6792, 2022.
15. Hamadou, B., R. Z. Falama, C. Delattre, G. Pierre, P. Dubessay, and P. Michaud, "Influence of physicochemical characteristics of neem seeds (Azadirachta indica A. Juss) on biodiesel production," *Biomolecules*, Vol. 10, 2020.
16. Madiwale, S. and V. Bhojwani, "An overview on production, properties, performance and emission analysis of blends of biodiesel," *Procedia Technology*, Vol. 25, 2016.